

FULL-POTENTIAL FLOW COMPUTATIONS USING CARTESIAN GRIDS

S.S.Desai, R.Rangarajan, J.P.Singh and K.S.Ravichandran
Scientists, Aerodynamics Division
National Aeronautical Laboratory, Bangalore. India

ABSTRACT

The main thrust of this paper has been the exploitation of Cartesian grids in the numerical solution of transonic full potential equation. Notwithstanding the present-day popularity for the use of body-wrapped coordinate systems in the context of Computational Fluid Dynamics, concerted effort has been made here to work with Cartesian grids for a variety of flow situations: aerofoils, axisymmetric flows, wings and wing-body combinations. One reason for this is that the codes based on these grids become amenable to computers with limited storage and speed. Several cases are presented here for each of the above flow situations. The results clearly demonstrate the efficacy of Cartesian grids for dealing with complex geometries and also underscore their use in the design of computer codes usable as engineering tools.

1. INTRODUCTION

It has now become a common practice to compute flow past 2D and 3D bodies in body-fitted coordinates. Presently there are fast grid generating routines available for 2D cases, but such an attempt for 3D geometries still remains a complex task and results in expensive flow solving procedures. There have been a few attempts, albeit by a minority, to revert back to Cartesian grids to solve 2D and 3D problems using full potential and Euler equations. Transonic full potential calculations in stretched Cartesian grids have been carried out earlier by Carlson¹ for both analysis and design of aerofoils and recently by Carlson and Weed² for the transonic analysis and design of wing. Wedan and South³ have used the Cartesian grid together with a finite volume approach for flows past lifting and non-lifting bodies. More recently Clarke et al⁴ have extended the method of Ref.3 to obtain Euler solutions for flow past multi-element aerofoils.

At the National Aeronautical Laboratory, (NAL), Bangalore, India, there has been a similar effort to see if Cartesian grids can be effectively used to solve various flow problems. Successful codes have already been written and good results have been obtained for: (a) transonic inviscid 2D flow in both analysis and design modes^{5,6}, (b) transonic viscous 2D flow with wake effects^{7,8}, (c) low speed flow past aerofoils at high incidence with separation⁹, (d) axisymmetric flows¹⁰, (e) inviscid 3D flows past wings and wing-body combinations^{11,12}, and recently (f) solution of 2D Euler equations¹³.

Computations using body-conforming grids, while being relatively simple and inexpensive for 2D cases, impose a heavy overhead on computer for flow calculation for 3D geometries: more core is needed to store the Jacobian and the metric coefficients and more arithmetic operations are involved while solving the transformed governing equations. As a reward, of course, one achieves ease of implementation of the surface boundary conditions and the consequential accuracy in the final numerical solution. However, if the latter result can be achieved at the cost of some additional analysis and coding effort, the Cartesian grid approach promises to be of considerable value, particularly in those situations where computer core availability is limited. But it should be mentioned here that the additional analysis and care is not a penalty restricted to Cartesian grids alone, because complex body-conforming grids do also require careful handling at singular points, fines and surfaces in the coordinate transformations, which in no way can be avoided for complex 3D geometries.

The experimentation at the National Aeronautical Laboratory with computations using Cartesian grids have demonstrated that the results for the 2D and the axisymmetric flows are as good as those that use more sophisticated grids and that the approach⁴ is very promising for the 3D configurations, particularly for engineering purposes of design and development. While more work is in progress, the experience already gained indicates that the apparent simplicity and economy of the method does not necessarily force one to compromise on the quality of computed results. In fact, this study at NAL is revealing and also so promising that we have little hesitation in agreeing with South⁵ when he suggests that the "rectangular grids may provide the best alternative for complex configurations." This paper aims to summarize the work carried out at the National Aeronautical Laboratory, Bangalore, India, over the past few years to solve transonic full potential equation in a Cartesian framework, with particular emphasis on the recent work on transonic wing and wing-body computations.

2. GOVERNING EQUATIONS, STRETCHED CARTESIAN GRIDS AND THE BOUNDARY CONDITIONS2.1 GOVERNING EQUATIONS

The 3D full potential equation governing inviscid transonic flows with weak shocks is

REPRODUCIBILITY OF THE ORIGINAL PAGE IS POOR

given in terms of the perturbation potential ϕ , in a stretched Cartesian grid $\xi = \xi(x)$, $\eta = \eta(y)$, $\zeta = \zeta(z)$, in the form

$$\begin{aligned} & (\bar{a}^2 - U^2)(f\phi_\xi)_\xi + (\bar{a}^2 - W^2)(h\phi_\zeta)_\zeta - 2UW(fh\phi_{\xi\zeta}) \\ & + (\bar{a}^2 - V^2)(g\phi_\eta)_\eta - 2UVfg\phi_{\xi\eta} - 2VWgh\phi_{\eta\zeta} + \\ & \delta h\phi_\zeta / \zeta = 0 \quad (I) \end{aligned}$$

where

$$\phi = M_\infty (x \cos \alpha + z \sin \alpha + \phi)$$

$$\bar{a}^2 = a/a_\infty = (1 - \frac{\gamma-1}{2}(U^2 + V^2 + W^2 - M_\infty^2))^{1/2}$$

$$U = M_\infty (\cos \alpha + f\phi_\xi),$$

$$V = M_\infty g\phi_\eta$$

$$W = M_\infty (\sin \alpha + h\phi_\zeta)$$

$$f = d\xi/dx, \quad g = d\eta/dy, \quad h = d\zeta/dz$$

a = speed of sound

α = angle of incidence (zero for axisymmetric flow)

Equation (1) applies to 2D and axisymmetric flows when all the terms involving η -derivatives are dropped. Further $\delta = 0$ for 2D and 3D flows and $\delta = 1$ and $\alpha = 0$ for axisymmetric case.

2.2 STRETCHED CARTESIAN GRID

The infinite physical space (x, y, z) is transformed into finite computational space (ξ, η, ζ) by a set of three mutually independent stretchings given below (See Fig.1).

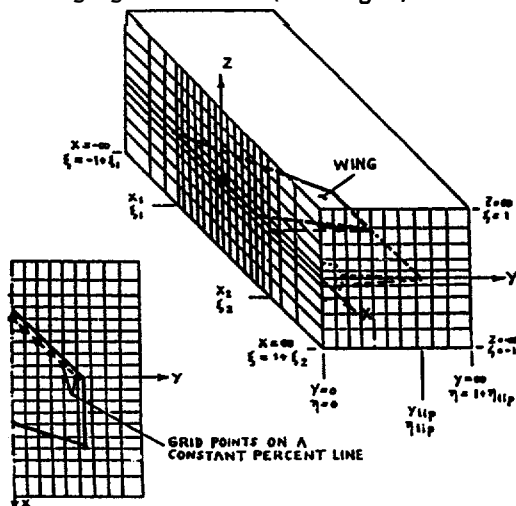


Fig.1 : STRETCHED CARTESIAN GRID

(i) x - ξ stretching

The region $-\infty < x < \infty$ is divided into three regions:

REGION I: $-\infty < x \leq x_1 \longleftrightarrow (-1+\xi_1) \leq \xi \leq \xi_1$

$$x = x_1 + A_2 \tan(\pi/2(\xi - \xi_1)) + A_3 \tan(\pi/2(\xi - \xi_1)^3)$$

REGION II: $x_1 \leq x \leq x_2 \longleftrightarrow \xi_1 \leq \xi \leq \xi_2$

$$x = a\xi + b\xi^2$$

REGION III: $x_2 \leq x < \infty \longleftrightarrow \xi_2 \leq \xi \leq 1+\xi_2$

$$x = x_2 + A_2 \tan(\pi/2(\xi - \xi_2)) + A_3 \tan(\pi/2(\xi - \xi_2)^3)$$

x_1 is located close to the leading edge (typically 1% of the length of the axisymmetric body, or 1% of the chordline for aerofoils and wings). $x_2 = -x_1$ for 2D and axisymmetric cases. The parameters ξ_1 and ξ_2 are subject to the requirement that (a) the number of grid lines over the aerofoil or the extent of the wing in the x -direction is equal to a specified fraction (typically 2/3) of the total number of x -grid lines, and (b) that the first grid point just behind the leading edge for a given wing planform be at a specified constant percent of the local chord (typically 8%). The latter requirement is easily met for straight wings but requires some attention for swept wings¹⁴. For 2D and axisymmetric cases $\xi_1 = \xi_2$. The parameters a and b are determined by the requirement of continuity of the mapping and its first derivative at the junction points x_1 and x_2 , while A_2 and A_3 are the free parameters set to $A_2 = 0.15$, $A_3 = 3.87$ following Carlson¹. For 3D cases b is set to zero with a view to satisfying the requirement (b) above.

(ii) z - ζ stretching

$$z = A_1 \tan(\frac{\pi}{2}\zeta) + A_4 \tan(\frac{\pi}{2}\zeta^3)$$

where A_1 and A_4 determine the spacing of the 2-grid lines near $z = 0$ and infinity, respectively. For cases with shocks extending into the far field, we need to use A_4 between 1 and 2; otherwise A_4 can be set to zero. A_1 is chosen such that there is exactly one grid point between the contour and the $y = 0$ line on the first $x = \text{constant}$ line through the nose. Generally $A_1 = 0.246$ for 2D and 3D cases; for axisymmetric cases A has been varied between 0.08 and 0.3510.

(iii) Y - η stretching (for 3-D only)

$$\begin{aligned} y &= C\eta, \quad 0 \leq y \leq y_{tip} \\ &= y_{tip} + C \tanh^{-1}(\eta - \eta_{tip}), \quad y_{tip} \leq y < \infty \end{aligned}$$

The above function maps $0 \leq y < \infty$ to $0 \leq \eta \leq 1 + \eta_{tip}$. The parameter tip , corresponding to y_{tip} , is determined by the fraction of the total number of grid lines required to fall on the wing. C is determined by the requirement of continuity of the stretching across the y_{tip} line.

2.3 BOUNDARY CONDITIONS

(a) Far field boundary conditions (Fig.2)

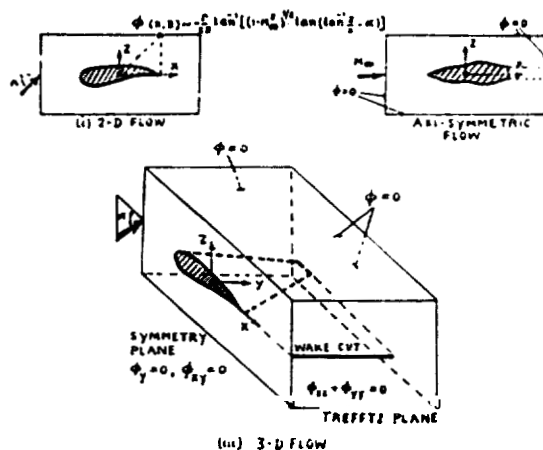


Fig.2 : FAR-FIELD BOUNDARY CONDITIONS

(i) 2-D flows

Here the far field corresponds to the potential of a single vortex of strength Γ placed at the origin of coordinates

$$\phi = \frac{\Gamma}{2\pi} \tan^{-1} \left((1-M_\infty^2)^{1/2} \tan(\tan^{-1}(y/x) - \alpha) \right)$$

where Γ is consistent with the Kutta condition.

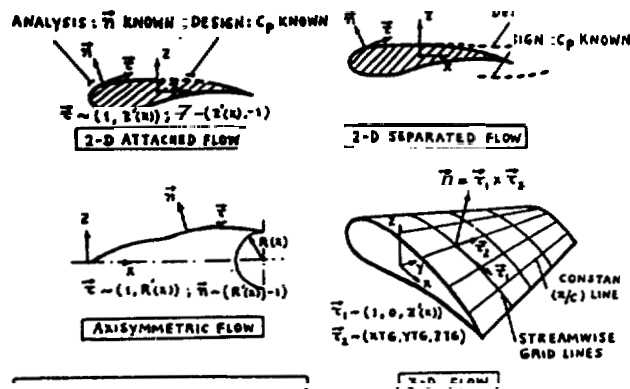
(ii) Axisymmetric flow

Here $\phi \equiv 0$ on all the far field boundaries.

(iii) 3-D flows

$\phi \equiv 0$ on all the far field boundaries except the Trefftz plane. $X \rightarrow \infty$, where a solution of the Laplace equation is obtained satisfying the jump condition across the wake corresponding to the jump in ϕ at the trailing edge at each spanwise location.

(b) Surface Boundary Conditions (Fig.3)



SUMMARY OF SURFACE BOUNDARY CONDITIONS
ANALYSIS: $\vec{r} \cdot \vec{n} = 0$, INVISCID
DESIGN: $\vec{n} = \vec{n}(U_b, V_b, W_b, C_p)$

Fig.3 : SURFACE BOUNDARY CONDITIONS

The surface tangency condition is a statement at the body surface on $\vec{q} \cdot \vec{n}$ for analysis (direct) and on C_p for design (inverse) problem. In the Cartesian coordinate system this can only be satisfied by using a Taylor series expansion since the body contour does not necessarily pass through the grid points. This is one of the main difficulties, as also often a source of error, in the Cartesian formulation. In our formulation, the boundary conditions are expanded in a Taylor series around the first grid point outside the body. The statement on $\vec{q} \cdot \vec{n}$ or $\partial\phi/\partial n$ then determines the potential value of ϕ at the first 'dummy' point (see figure below). It may be mentioned here that the determination of this dummy value is a simple matter when the coordinate system is body-fitted and orthogonal.

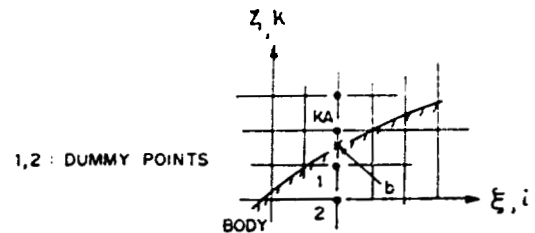


Fig.4 : APPLICATION OF SURFACE TANGENCY IN CARTESIAN GRID

Another difficulty is that a source of instability arises whenever the flow at the first field point outside the body happens to be supersonic and the W-component of velocity has direction from inside to the outside of the body ($W > 0$ for upper surface and $W < 0$ for lower surface, respectively). While using rotated differencing we then need the value of ϕ at the second dummy point. One can use a linear extrapolation for the value of ϕ at the second dummy point: $\phi_2 = -\phi_{KA} + 2\phi_1$

This linear extrapolation was used in the initial stage for 2-D code development and was found to be the source of instability. Actually, the above linear extrapolation incorrectly restricts $\phi_{\zeta\zeta}$ to vanish at the first field point outside the body when it is approximated by backward differencing in a rotated differencing scheme. In the 2-D and the 3-D codes we avoid the instability by a (compensative) explicit addition of the second derivative $\phi_{\zeta\zeta}$ at KA, now obtained through centered differencing at KA (instead of the backward differencing)

$$\phi_{\zeta\zeta} \text{ at KA} = \frac{\phi_{KA+1} - 2\phi_{KA} + \phi_1}{(\Delta\zeta)^2}$$

In the axisymmetric code the extrapolation

$$\phi_2 = 2.5\phi_1 - 2\phi_{KA} + 0.5\phi_{KA+1}$$

has given better results, as this extrapolation does not force ϕ_{55} to vanish at KA.

This feature of the extrapolation is retained for the design mode also, where now the prescribed C_p determines the modified normal to the body surface rather than the given normal determining the expression $\vec{q} \cdot \vec{n}$. This design mode is used in modifying a given aerofoil surface according to a prescribed pressure distribution as also in determining the force free surface emanating from an assumed separation point with the $C_{p,sep}$ given by

$$C_{p,sep} = -2 (\phi_{ITE} - \phi_{sep}) / (X_{ITE} - X_{sep})$$

where ITE refers to the last grid location just inside the trailing edge and X_{sep} is the location of the point of separation.

3. ROTATED TYPE-DIFFERENCING AND THE SUCCESSIVE OVER-RELAXATION

DISCRETIZATION

The discret procedure employed in all the cases presented here conforms to the outline prescribed used in transonic flow computation. The main features are

(i) Central differencing at all subsonic grid points wherein the equation written in the stretched Cartesian grid is used for the discretization.

(ii) Rotated differencing scheme at all supersonic points. Here the governing equation is written in streamline (s,n) coordinate system to facilitate (a) retarded differencing of all the derivatives contributing to the streamwise derivatives and (b) centred differencing for all the derivatives contributing to the derivatives normal to the streamline directions,

(iii) Suitable mixing of the old and the new values of ϕ so that the time derivative terms ϕ_{nt} are simulated and

(iv) Adding explicitly a ϕ_{st} term to make the iterative procedure stable (See Jameson¹⁷). These details can be seen in Carlson¹, Rangarajan and Desai⁵ for the 2D cases and in Desai, Rangarajan and Ravichandran¹¹ for the 3D case.

3.2 SOLUTION PROCEDURE

The discretization of the governing equation and the boundary conditions leads to a system of simultaneous equations for the potential ϕ at the field points of the discretized flow domain. For the 2D and the axisymmetric flows these equations are solved by successive line relaxation starting from upstream infinity and sweeping to the

downstream infinity. In each of these lines a tridiagonal matrix equation is solved using Thomas algorithm.

In the 3D case the above computation is performed in each x-z plane beginning from the plane of symmetry (y = 0) and moving outwards spanwise.

The iterative procedure proceeds from a zero-field for the potential and is continued till a prescribed convergence is reached

$$\text{Max}_{l,j,k} (\phi_{l,j,k}^{n+1} - \phi_{l,j,k}^n) < \epsilon$$

For 2D and axisymmetric flows: $\epsilon \sim 1 \times 10^{-5}$ and for 3D it is generally 0.5×10^{-4} .

It is found to be computationally economical to carry out the calculations on a sequence of three grid levels.

TABLE

CASE	CORE * (K words)	CPU (Mins) *
2D code (viscous)	40	1 - 4
Axisymmetric	40	0.5 - 15
3D wing	110	150, single grid 40, grid sequencing (3 levels)
3D wing-body	140	

* UNIVAC 1100/60-C1 ($\sim 0.3 \text{MFLOPS}$)

4. VISCOUS CORRECTIONS

Boundary layer and wake parameters for a given pressure distribution, obtained during potential flow solution, are computed following the method of Green et al¹⁸. A fourth-order Runge-Kutta scheme is used to integrate the two integral boundary layer equations together with an integral kinetic energy equation (Desai and Kiske¹⁹).

The viscous corrections for the 2D case are fully implemented using the transpiration model for both the boundary layer and the wake; viscous ramp is also included to simulate the effects of strong shock. For the 3D case these corrections are carried over but in the absence of thorough validation, only inviscid results are presented here.

5. RESULTS AND DISCUSSIONS

5.1 2D ATTACHED FLOWS

Fig.5 brings out the comparison of the present inviscid results with other inviscid numerical results presented at the GAMM Workshop 20. Comparison is made here particularly for flow conditions where shock is considerably strong. The prediction of the position of shock is remarkably close to that from Euler solution of Rizzi for both the cases. The prediction of peak negative pressures and the strength of the shock is also comparable with the predictions from Euler solutions.

A few viscous calculations are their comparison with the available experimental results are brought together in Fig.6. The comparisons for the NACA 0012 aerofoil for pressure distribution²¹ is quite good both for subcritical (Fig.6a) and supercritical (Fig.6b) cases. The lift curve slope comparison shown in Fig.6c clearly brings out the usefulness of the code as an engineering tool. Fig.7 shows the comparison of present results with the experiments²² for the RAE 2822 aerofoil. Good comparisons are also seen with available experimental boundary layer parameters. In Fig.7c we have the comparisons made for a rather stringent case of the RAE 2822 where the poor recovery of the experimental trailing edge pressures shows imminent separation. The viscous ramp model seems to improve the shock location but the good comparison of the pressures downstream of the shock obtained without the viscous ramp is now disturbed. Only a few comparisons are shown here just to bring out the capability of the method: for a large number of comparisons, reference may be made to Desai and Rangarajan³.

5.2 2D DESIGN

Three cases of transonic design of aerofoils⁶ using the present method are shown in Fig.8. The consistency of the design procedure is shown in Figs.8a and 8b, where the NACA 0012 aerofoil is modified for shockless conditions and thin modified aerofoil is remodified to NACA 0012 by suitably prescribing this target pressure distribution. Fig.8c shows the modifications to a 5% thick MCA 65,4005 aerofoil corresponding to a shockfree target pressure distribution.

5.3 2D LOW SPEED SEPARATED FLOW

A combination of the viscous analysis up to the separation point and the inverse procedure beyond the separation point corresponding to the prescribed constant pressure level (equal to C_p at separation point), gives an ability to predict separated flows. Presently only the low speed separated flows can be handled. Fig.9 brings out the comparison with experiments for two aerofoils. The comparison is seen to be quite good.

5.4 AXISYMMETRIC FLOW

Comparisons between inviscid computations and experiments for two axisymmetric bodies are shown in Fig.10. The comparisons shown in Figs.10a to 10c are reasonably good over the entire length of the body. Viscous corrections have been implemented in this code but results are not presented here.

5.5 3D COMPUTATIONS; WING ALONE CASES

Results of the transonic computations for four different wings are compared in Figs.11 to 14 with the available experimental and other numerical results.

Before discussing the results further, a comment is in order regarding the freestream Mach number and incidence used in the present computations and the question of wind tunnel wall corrections. In the cases presented here, wherever corrections have been used in Mach number and the angle of attack, they have been explicitly so indicated but these corrections do not necessarily conform to those used by other workers. It is a fact well known now that for comparable pressure distributions not only the Mach number and incidence have to be different between two wind tunnels, but also that "separate corrections tailored to each individual computer code may be required"²³.

This fact will have to be borne in mind while assessing some of the results for 3D flows presented here.

The results for the standard case of ONERA M-6 wing with $M_\infty = 0.84$, $\alpha = 3.06^\circ$ are compared with experiment in Fig.11. The agreement is seen to be satisfactory.

In Fig.12 results and comparison with NAL experiments are presented for a generic wing of $AR = 3.6$, sweep = 43.33° , with an RAE section. As can be seen, the comparison here is quite good.

Fig.13 gives results for the LOCKHEED wing-A;²⁴ There is a similarity between the results from FL022 code, except for the shock locations, at all spanwise stations. It seems that such discrepancies can be reconciled with a stripwise viscous correction as is demonstrated recently by Carlson and Weed² for the same case.

Results for LOCKHEED wing-C are presented in Fig.14. This is a case of a wing which involves considerable twist. For this case a fair comparison has been obtained with experiments.

finally, results are presented in Fig.15 for a wing-body combination L51F07 of reference 25. The present results are compared with the experiments and also with the numerical results of Boppe 26. There is an overall good agreement between the experiments and the present numerical results. As with the cases presented before, the shock is found to be downstream of the experimental location in the outboard region. Here too viscous effects may play a vital role. Particularly noteworthy is the close agreement between the theory and the experiments for the body pressures on the meridional plane.

5.7 SOME COMMENTS ON WING AND WING-BODY COMPUTATIONS

In all the cases presented here the comparison towards the outboard 20% of the span deteriorates. This is due to the fact that in a Cartesian grid, number of grid points on the tip region decreases with the taper ratio for a given total number of grid lines in the streamwise direction; for example with about 60 grid points in the root section there can hardly be 20 points on the tip region for a wing with a taper ratio of 1/3. Consequently the resolution of the flow field deteriorates towards the tip. The technique of grid-embedding, so successfully employed by Boppe 26 seems to provide a solution to this problem. Currently efforts are being made in this direction.

Viscous interaction, as a first step in the form of two-dimension strip method, will be a second element for further improving the present results. Recently viscous corrections have been incorporated into the wing and wing-body codes using a transpiration model for the viscous effects. Green's 18 Lag entrainment method is used for the two-dimensional boundary layer parameters at each spanwise station. This code is presently under validation studies.

6. CONCLUSIONS

In summary, the following conclusions are drawn from the present study.

(i) Efficient and accurate codes can be written in the frame work of stretched Cartesian grids to deal with a variety of flows: aerofoils, axisymmetric bodies, wings and wing-body combinations, both in design and in analysis mode.

(ii) These codes require less computer storage. They therefore are suited to situations where supercomputers are not available. and provide the only means of obtaining results of engineering accuracy on smaller computers.

ACKNOWLEDGE

It is our pleasure here to acknowledge the encouragement for this work from Prof. R. Narasimha, Director and Mr. M. Shivakumara Swamy, Head, Aerodynamics Division, National Aeronautical Laboratory. The assistance from the Drawing Office in the preparation of figures and from Ms. M. Manjula in the meticulous typing is also gratefully acknowledged. The initial phase of the present work was funded from the Aeronautics Research and Development Board (AR&DB), India.

REFERENCES

01. CARLSON, L.A.: Transonic analysis and design using Cartesian coordinates, J. Aircraft, Vol.13, No.5, pp. 342-356, 1976.
02. CARLSON, L.A., WOOD, R.A.: Direct-inverse transonic wing analysis - Design method with viscous interaction, J. Aircraft, Vol.23, No.9, September, 1976.
03. WEDAN, B., SOUTH, J.C.: A method for solving the transonic full potential equation for general configurations, AIAA paper 83-1889, 1983.
04. CLARKE, D.K., SALAS, M.D., HASSAN, H.A.: Euler calculations for multi-element aerofoils using Cartesian grids, AIAA J. Vol.24, No.3, March 1986.
05. RANGARAJAN, R., DESAI, S.S., RAMASWAMY, M.A.: 2D transonic analysis and design program in Cartesian coordinates (TRADE 1), NAL AE-TM-6-83, September 1983.
06. RANGARAJAN, R.: Analysis and design of supercritical aerofoils, M.Sc. Thesis, Dept of Aerospace Engg, Indian Institute of Science, Bangalore, January 1986.
07. DESAI, S.S., RANGARAJAN, R.: Prediction of viscous effects on an aerofoil using transpiration model for the effects of boundary layer and wake, NAL TM AE 8609, August 1986.
08. DESAI, S.S., RANGARAJAN, R.: Viscous transonic flow over aerofoils using transonic full potential equation in a system of Cartesian coordinates, AIAA paper No. 87-0411, AIAA 25th Aerospace Sciences Meeting, Reno, Nevada, 12-15 January 1987.
09. SINGH, J.P., RANGARAJAN, R., RAMASWAMY, M.A.: Computation of flow over aerofoil under high lift separated flow conditions, NAL PD AE 8531, December 1985.
10. SINGH, J.P.: Inviscid axisymmetric transonic flow computation in Cartesian coordinates, NAL AE-TM-1-84, August 1984.
11. DESAI, S.S., RANGARAJAN, R., RAVICHANDRAN, K.S.: A preliminary note on the development of a three-dimensional potential code in Cartesian coordinates, NAL TM AE 8504, July 1985.

12. DESAI, S.S., RANGARAJAN, R., RAVICHANDRAN, K.S.: Three-dimensional transonic full potential code in Cartesian coordinates, Paper 481-4, 3rd ACFM, Tokyo, Japan. 1-5 September 1986.
13. DESAI, S.S., SINHA, U.N., RANGARAJAN, R.: Solution of 2D Euler equations in Cartesian coordinates. in preparation.
14. RAVICHANDRAN, K.S., DESAI, S.S., RANGARAJAN, R.: Modification to the Cartesian grid in 3D potential code for flow past swept wings, VAL PD AE 8615, June 1986.
15. SOUTH, J.C.: Advances in Computation Transonics, Vol.4, 1985.
16. CARLSON, L.A., ROCHOLL, B.M.: Application of direct-inverse techniques in aerofoil analysis and design. NASA CP 2045, 1978.
17. JAMESON, A.: Iterative solution of transonic flows over airfoils and wings including flows at Mach 1, Communications on Pure and Applied Mathematics, Vol.27, PP.283-309. 1974.
18. GREEN, J.E., WEEKS, D.J., BROOMAN, J.W.F.: The prediction of turbulent boundary layers and wakes in compressible flow by a Lag entrainment method, RAE R&M 3791. 1973.
19. DESAI, S.S., KISKE, S.: A computer program to calculate turbulent boundary layers and wakes in compressible flows with arbitrary pressure gradient based on Green's Lag entrainment method, Bericht Nr.89/1982, Inst fur Thermo-u Fluidodynamik, Ruhr University, Bochum, 1982.
20. VIVIAND, H., RIZZI, A. (Eds): Numerical methods for computation of inviscid transonic flows with shock waves; a GAMM Workshop, 1981
21. HARRIS, C.D.: Two-dimensional aerodynamic characteristics of the NACA 0012 aerofoil in the Langley 8-foot transonic pressure tunnel, NASA TM 81927, April 1981.
22. COOK, P.H., McDONALD, M.A., FIRMIN, M.C.P.: Aerofoil RAE 2822 pressure distributions and boundary layer and wake measurements. A6-1, A6-57, AGARD AR-138, Exptl. Database for Computer Program Assessment. May 1979.
23. SUBRAMANIAN, N.R., HOLST, T.L., THOMAS, S.D.: Recent applications of the transonic wing analysis computer code TWING, NASA TM 84283.
24. HINSON, B.L., BURDGES, K.P.: An evaluation of three dimensional transonic codes using new correlation tailored test data, AIAA paper 80-0003, 1980.
25. LOVING, D.L., ESTRABROOKS, B.B.: Transonic wing investigation in the Langley 8-ft high speed tunnel at high subsonic Mach numbers and at a Mach number of 12. NACA RM L51F07, Sept 1951.
26. BOPPE, C.W.: Transonic flow field analysis for wing-fuselage configuration. NASA CR 3243, May 1980.

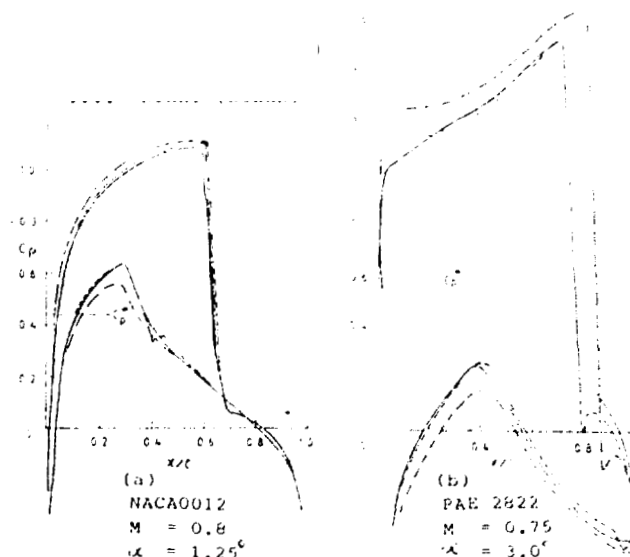


FIG. 5 INVISCID AEROFOIL RESULTS

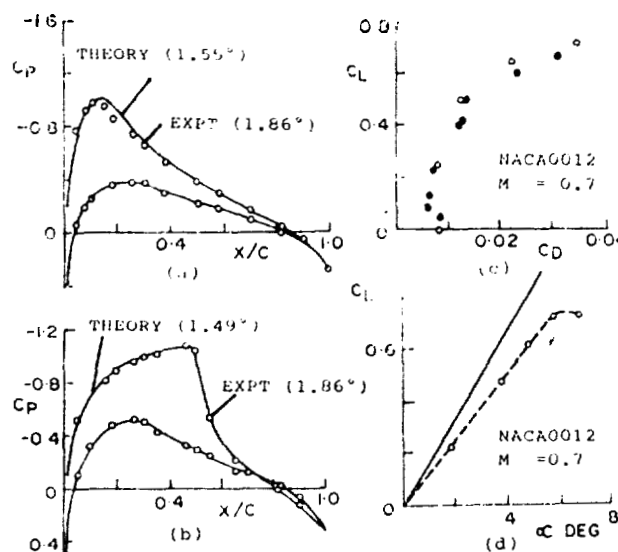


FIG. 6 VISCOUS AEROFOIL RESULTS : NACA0012

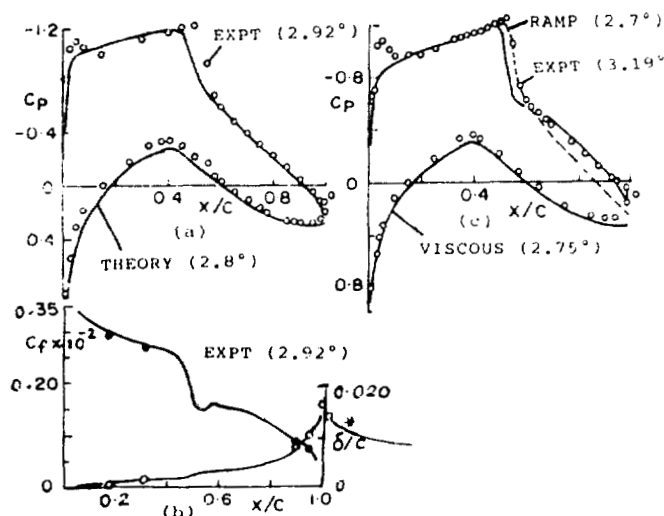
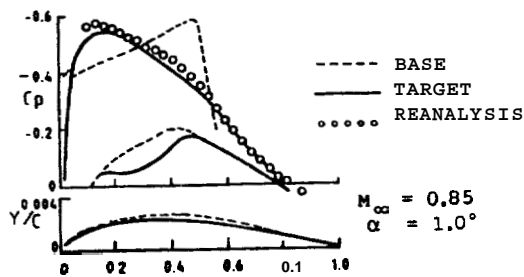
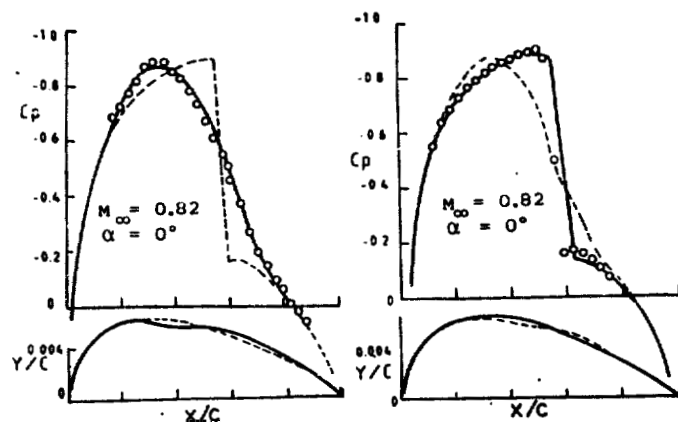


FIG. 7 VISCOUS AEROFOIL RESULTS : RAE2822



(c) DESIGN OF THIN AEROFOIL

FIG. 8 AEROFOIL DESIGN RESULTS

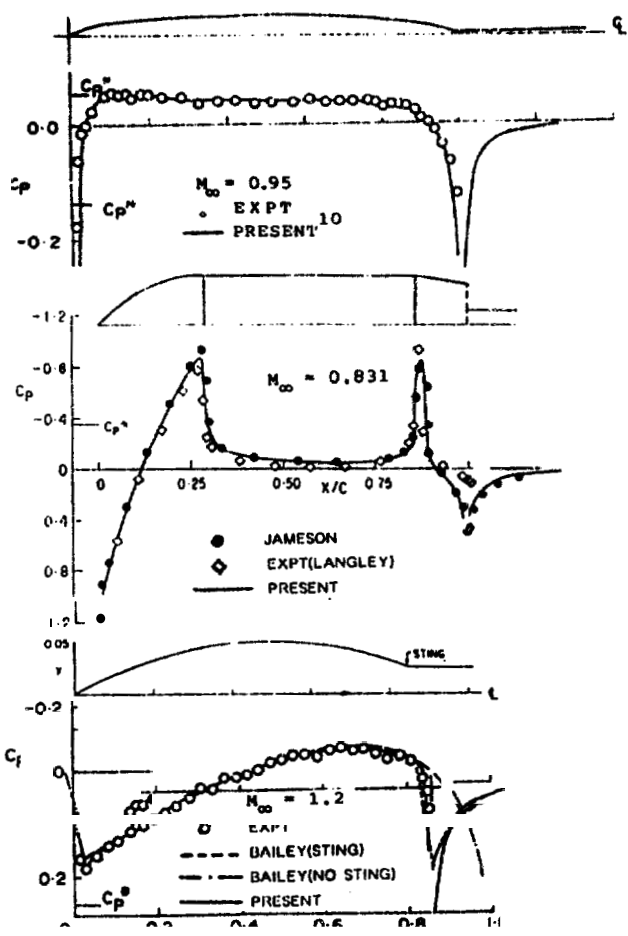


FIG. 10 AXISYMMETRIC FLOW RESULTS

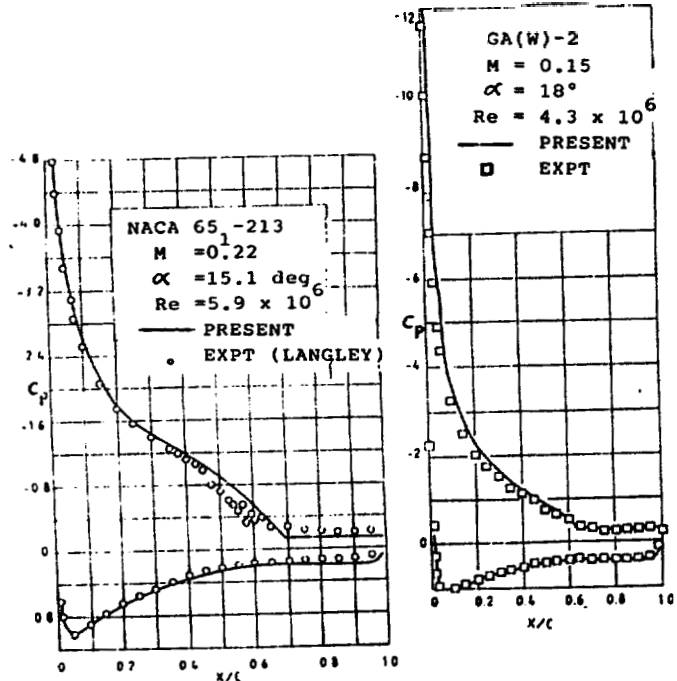


FIG. 9 LOW SPEED SEPARATED FLOW ON AEROFOILS

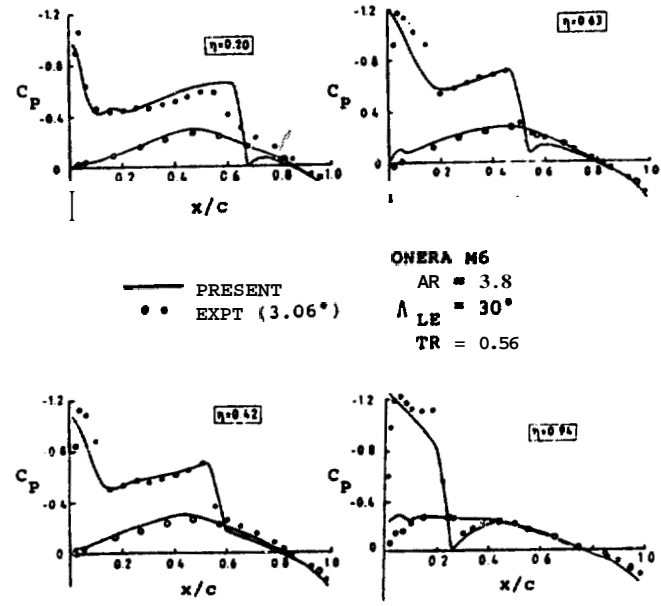


FIG. 11 INVISCID RESULTS FOR ONERA M6 WING
 $M = 0.84, \alpha = 3.06^{\circ}$

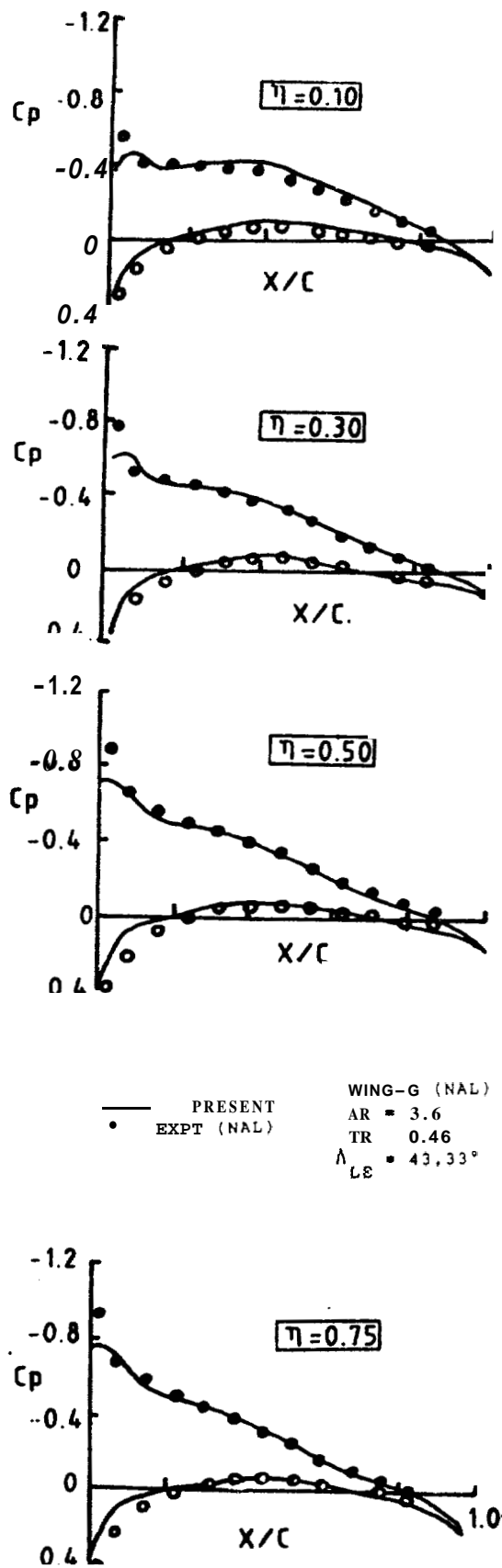


FIG. 12 INVISCID RESULTS FOR WING-G,
 $M = 0.7, \alpha = 5.0$

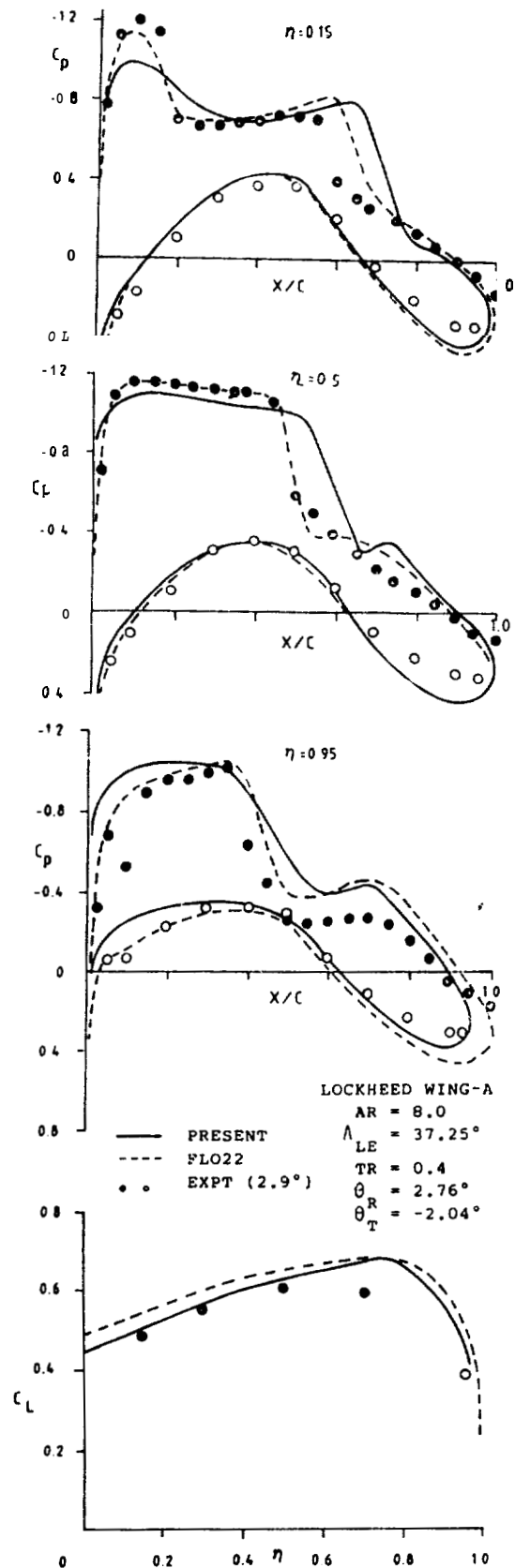


FIG. 13 INVISCID RESULTS FOR LOCKHEED
WING-A $M = 0.82, \alpha = 1.5^\circ$

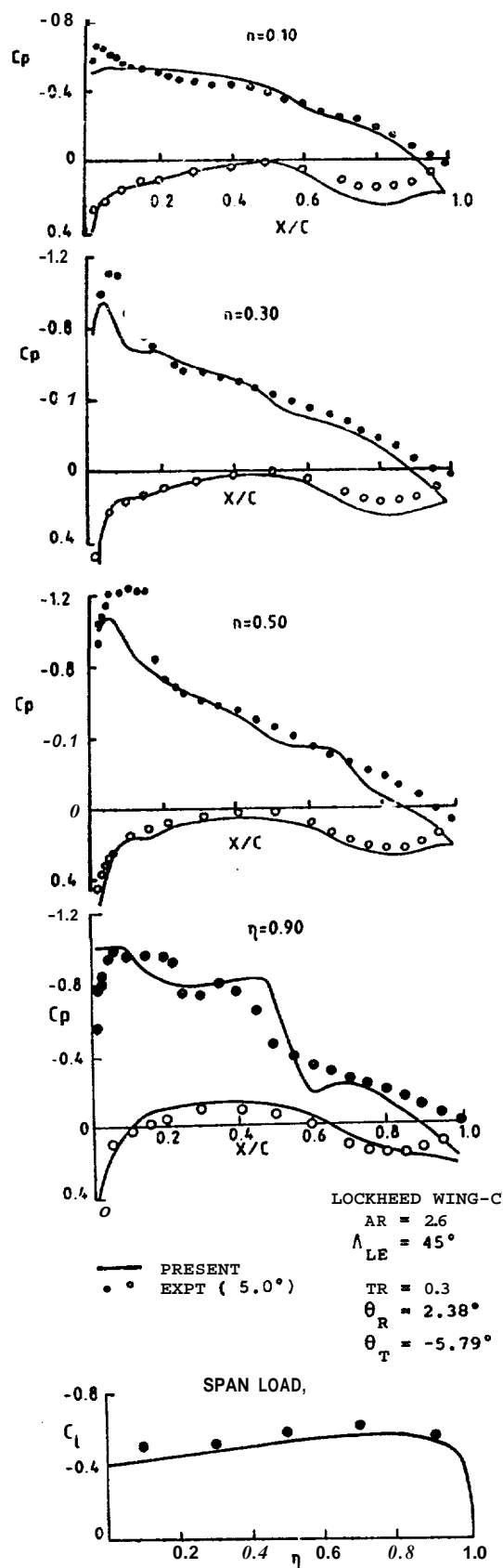


FIG. 14 INVISCID RESULTS FOR LOCKHEED WING-C
 $M = 0.82, \alpha = 6.0^\circ$

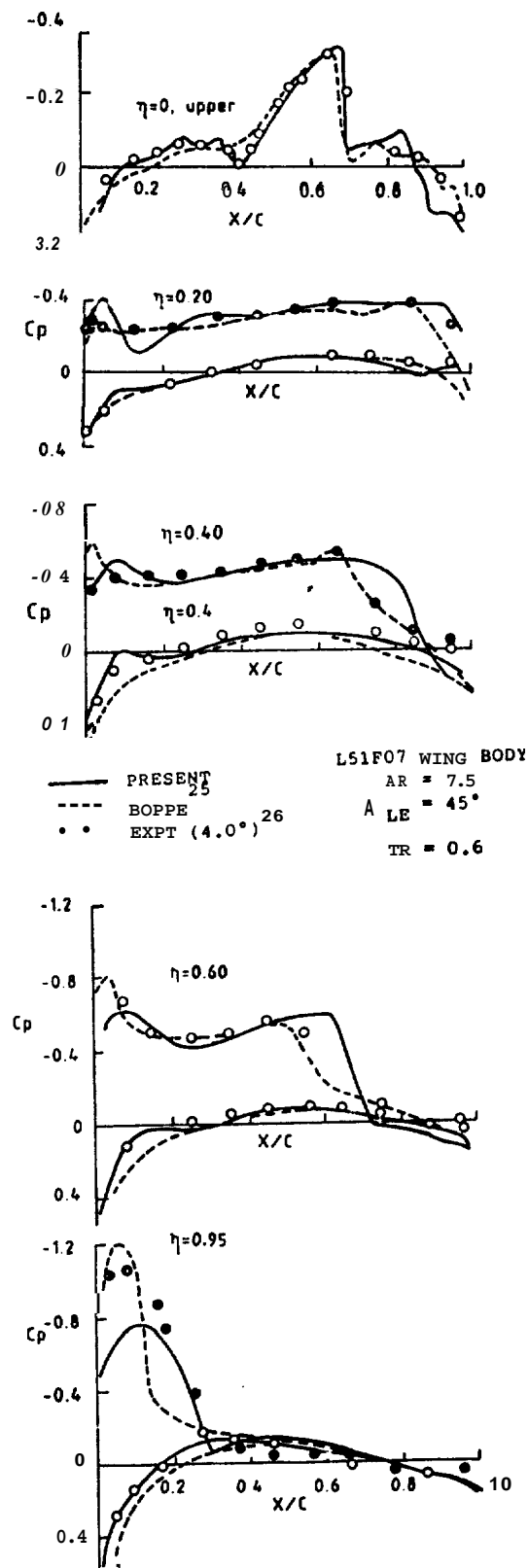


FIG. 15 INVISCID RESULTS FOR L51F07 WING-BODY
 $M = 0.93, \alpha = 4.0^\circ$

FULL-POTENTIAL FLOW COMPUTATIONS USING CARTESIAN GRIDS

S.S.Desai, R.Rangarajan, J.P.Singh and K.S.Ravichandran
Scientists, Aerodynamics Division
National Aeronautical Laboratory, Bangalore. India

ABSTRACT

The main thrust of this paper has been the exploitation of Cartesian grids in the numerical solution of transonic full potential equation. Notwithstanding the present-day popularity for the use of body-wrapped coordinate systems in the context of Computational Fluid Dynamics, concerted effort has been made here to work with Cartesian grids for a variety of flow situations: aerofoils, axisymmetric flows, wings and wing-body combinations. One reason for this is that the codes based on these grids become amenable to computers with limited storage and speed. Several cases are presented here for each of the above flow situations. The results clearly demonstrate the efficacy of Cartesian grids for dealing with complex geometries and also underscore their use in the design of computer codes usable as engineering tools.

1. INTRODUCTION

It has now become a common practice to compute flow past 2D and 3D bodies in body-fitted coordinates. Presently there are fast grid generating routines available for 2D cases, but such an attempt for 3D geometries still remains a complex task and results in expensive flow solving procedures. There have been a few attempts, albeit by a minority, to revert back to Cartesian grids to solve 2D and 3D problems using full potential and Euler equations. Transonic full potential calculations in stretched Cartesian grids have been carried out earlier by Carlson¹ for both analysis and design of aerofoils and recently by Carlson and Weed² for the transonic analysis and design of wing. Wedan and South³ have used the Cartesian grid together with a finite volume approach for flows past lifting and non-lifting bodies. More recently Clarke et al⁴ have extended the method of Ref.3 to obtain Euler solutions for flow past multi-element aerofoils.

At the National Aeronautical Laboratory, (NAL), Bangalore, India, there has been a similar effort to see if Cartesian grids can be effectively used to solve various flow problems. Successful codes have already been written and good results have been obtained for: (a) transonic inviscid 2D flow in both analysis and design modes^{5,6}, (b) transonic viscous 2D flow with wake effects^{7,8}, (c) low speed flow past aerofoils at high incidence with separation⁹, (d) axisymmetric flows¹⁰, (e) inviscid 3D flows past wings and wing-body combinations^{11,12}, and recently (f) solution of 2D Euler equations¹³.

Computations using body-conforming grids, while being relatively simple and inexpensive for 2D cases, impose a heavy overhead on computer for flow calculation for 3D geometries: more core is needed to store the Jacobian and the metric coefficients and more arithmetic operations are involved while solving the transformed governing equations. As a reward, of course, one achieves ease of implementation of the surface boundary conditions and the consequential accuracy in the final numerical solution. However, if the latter result can be achieved at the cost of some additional analysis and coding effort, the Cartesian grid approach promises to be of considerable value, particularly in those situations where computer core availability is limited. But it should be mentioned here that the additional analysis and care is not a penalty restricted to Cartesian grids alone, because complex body-conforming grids do also require careful handling at singular points, fines and surfaces in the coordinate transformations, which in no way can be avoided for complex 3D geometries.

The experimentation at the National Aeronautical Laboratory with computations using Cartesian grids have demonstrated that the results for the 2D and the axisymmetric flows are as good as those that use more sophisticated grids and that the approach⁴ is very promising for the 3D configurations, particularly for engineering purposes of design and development. While more work is in progress, the experience already gained indicates that the apparent simplicity and economy of the method does not necessarily force one to compromise on the quality of computed results. In fact, this study at NAL is revealing and also so promising that we have little hesitation in agreeing with South⁵ when he suggests that the "rectangular grids may provide the best alternative for complex configurations." This paper aims to summarize the work carried out at the National Aeronautical Laboratory, Bangalore, India, over the past few years to solve transonic full potential equation in a Cartesian framework, with particular emphasis on the recent work on transonic wing and wing-body computations.

2. GOVERNING EQUATIONS, STRETCHED CARTESIAN GRIDS AND THE BOUNDARY CONDITIONS

2.1 GOVERNING EQUATIONS

The 3D full potential equation governing inviscid transonic flows with weak shocks is

REPRODUCIBILITY OF THE ORIGINAL PAGE IS POOR